Regular Article

PHYSICAL CHEMISTRY RESEARCH
Published by the
Iranian Chemical Society
www.physchemres.org
info@physchemres.org

Phys. Chem. Res., Vol. 10, No. 2, 195-209, June 2022
DOI: 10.22036/pcr.2021.294078.1934

Modified D-Glucofuranoses as New Black Fungus Protease Inhibitors: Computational Screening, Docking, Dynamics, and QSAR Study

M. Atiqur Rahman[a], M.M. Matin[a,*], A. Kumer[b], U. Chakma[c] and Md. Rezaur Rahman[d]

[a]*Bioorganic and Medicinal Chemistry Laboratory, Department of Chemistry, Faculty of Science, University of Chittagong, Chittagong, 4331, Bangladesh*

[b]*Department of Chemistry, European University of Bangladesh, Gabtoli, Dhaka, 1216, Bangladesh*

[c]*Department of Electrical and Electronic Engineering, European University of Bangladesh, Gabtoli, Dhaka, 1216, Bangladesh*

[d]*Department of Chemical Engineering and Energy Sustainability, Faculty of Engineering, Universiti Malaysia Sarawak, Jalan Datuk Mohammad Musa, Kota Samarahan, 94300, Malaysia*

(Received 8 September 2021, Accepted 26 September 2021)

Notable antimicrobial functionality was found with different sugar esters which were also reported to inhibit the multidrug resistant pathogens along with promising antimicrobial efficacy, and drug-likeness properties. Recent black fungus outbreak, especially in India, along with COVID-19 surmounted the death toll and worsened the conditions severely due to lack of appropriate drugs. Hence, several glucofuranose type esters 4-8 were screened against black fungus related protein (2WTP). These molecules, optimized by DFT, showed good chemical and biological reactivity values especially with pathogens along with satisfactory ADMET profiles. With the good *in vitro* antifungal activities, these compounds were subjected for molecular docking against the protein of mucormycosis's pathogens, known as black fungus, followed by calculation of inhibition constant, binding energy, and molecular dynamics of the protein-ligand complex. Also, logpIC_{50} or pIC_{50} was calculated regarding the data for QSAR study. The molecular docking showed that 5-8 had a good binding affinity (> -6.50 kcal mol^{-1}) while 7 (-8.00 kcal mol^{-1}) and 8 (-8.20 kcal mol^{-1}) possessed excellent binding affinity. The inhibition constant and binding energy of the compounds were found very lower among others with stable complexes in 5000 ns in molecular dynamics. Considering all the results, sugar esters 7 and 8 are found to have promising drug properties.

Keywords: Black fungus, Inhibition constant (Ki), QSAR, Molecular docking, Molecular dynamics, Sugar esters (SEs)

INTRODUCTION

Amongst the biomolecules carbohydrates are widespread in nature and involved in a plethora of biological activities [1]. In spite of good solubility and biological functions, several natural carbohydrate compounds possess relatively poor binding affinities [2] which indicated the necessity of their structural modification to improve applicability in various fields including drug candidates [3-5]. Modifications for acylation of their one or several hydroxyl groups resulted in the formation of carbohydrate esters, termed as sugar esters (SEs) [6-7], allowing these molecules to apply in diverse synthetic, biological, and pharmaceutical industries [8-11]. The SEs, thus produced, also exhibit enhanced chemical stability and these new compounds could replace their original carbohydrates for novel interaction with target enzymes carbohydrate for novel interaction with target enzymes showing significant biological interactions [12,13]. However, site selective synthesis of such esters has long been faced with several inherent challenges [14-16]. The major reason is due to the presence of many secondary hydroxyl groups with almost similar reactivity and produces a mixture of SEs instead of site selectivity [17]. During the

*Corresponding author. E-mail: mahbubchem@cu.ac.bd

last century, several suitable methods for selective and regioselective esterification were established and could be used based on of necessity [18-23].

Of the synthetic and natural SEs many glucofuranose esters of alkyl-fumarates were reported as suitable for the medication of hyper-proliferative, inflammatory or autoimmune disorders [24] and can control their solubility with different hydrophobic alkyl chains [25]. Protected glucofuranose like 1,2,5,6-di-*O*-isopropylidene-D-glucose has been used as an intermediate for the synthesis of many natural and synthetic novel bioactive compounds [26-28]. It was shown that 3-*O*-acyl glucofuranoses (Figs. 1a-c), as synthesized by Catelani *et al.* [29], have the potentiality to regularize uncontrolled cell growth in erythroid tumor cells. Similarly, seprilose type compounds (*e.g.* 2) are established as drugs [30,31]. Additionally, incorporation of alkyl and aromatic based acyl groups with glucofuranose and other sugar skeletons were reported to increase their antimicrobial potentiality especially antifungal efficacy [32-35] and the activities were in some cases comparable to the standard antibiotics.

Black yeast-like fungi provide fascinating applications in biotechnology, bioremediation, agriculture, or medicine, but it was thought that their infectious abilities might harm these efforts [36]. For example, Najafzadeh *et al.* [36] reported that black fungal infection caused brain disease in the cats. The observation comes true where recent reports of infections with mucormycosis, *i.e.* black fungus the cats. The observation comes true where recent reports of infections with mucormycosis, i.e. black fungus [37,38], in COVID-19 patients worsen the pandemic situation, especially in India. Concurrent attacks of black fungus and COVID-19 highly lowers the body's immune defenses [39]. Although some drugs like steroids were used in COVID-19 patients, black fungus reduces steroidal activity and further exacerbates the patient's immune system [40]. In general, this soil fungus when goes in through a cut or a burn, can cause local infections; when it enters through the sinus, it can affect the eyes and eventually, the brain, leading to a fatal situation [41]. New drugs for the treatment of both these infectious diseases are highly expected.

As mentioned earlier that SEs possess better antifungal activities their efficacy against black fungal protein was

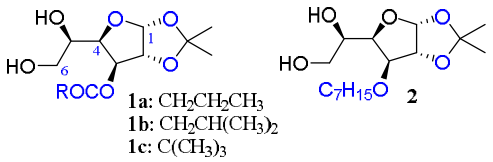

Fig. 1. Structure of glucofuranose ester 1 and 2.

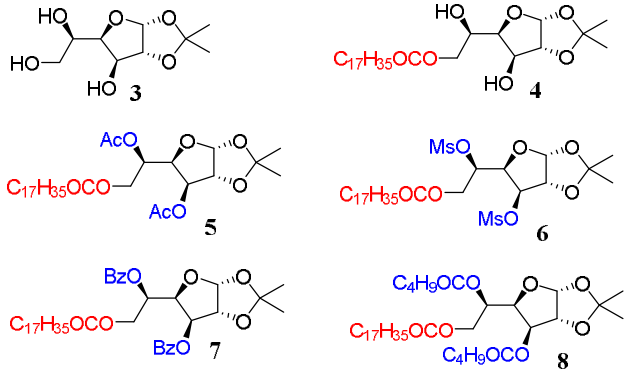

Fig. 2. Glucofuranose **3** derived esters 4-8.

studied computationally in considering the present situation. Glucofuranose 3 derived several SEs 4-8, as shown in Fig. 2, were previously synthesized, characterized, and tested against 10 human pathogenic bacteria and 7 fungi [42]. Some of these esters showed very well *in vitro* antifungal inhibition, which were comparable to that of the standard antibiotic fluconazole [42]. Thus, it is very much reasonable to study their binding affinity and binding energy against mucormycosis's pathogens (black fungus; PDB ID: 2WTP) along with frontier molecular orbitals (FMO), chemical descriptors, drug-likeness, and ADMET properties.

EXPERIMENTAL

Preparation of Ligand and Calculation of Chemical Reactivity and Descriptors

The DFT (density functional theory) functional was used for molecular optimization using the method vibrational frequency from the DMol code of material studio 08 [43-45]. During the setting of the functionals in DMol code, the B3LYP functional and 6-31G++ basis set were used to get highly accurate results due to having the electronegative atom oxygen. After optimization, the analysis tools were used to design the frontier molecular orbitals (HOMO and

LUMO), and the magnitude of HOMO, LUMO. The optimized molecular structures were saved for further computational work, such as molecular docking, molecular dynamic, and ADMET as pdf files. The magnitude of chemical reactivity and descriptors are calculated using related accepted equations. Such as- energy gap, $\Delta\varepsilon = \varepsilon_{LUMO} - \varepsilon_{HOMO}$; ionization potential, $I = -\varepsilon_{HOMO}$; electron affinity, $A = -\varepsilon_{LUMO}$; electronegativity, $\chi = (I + A)/2$; chemical potential, $\mu = -(I + A)/2$; hardness, $\eta = (I - A)/2$; electrophilicity, $\omega = \mu^2/2\eta$; softness, $S = 1/\eta$.

Determination of the Data of ADMET and Lipinski Rule

Before the molecular docking study, the selected drugs were run on SwissADME online database (http://www.swissadme.ch) [46] for evaluating their Lipinski rule satisfaction. After full satisfaction of Lipinski rule, these were selected for molecular docking study. Besides, the ADMET properties were completed by the online database amdetSAR (http://lmmd.ecust.edu.cn/admetsar2) which is the most acceptable database for predicting the AMDET (absorption, distribution, metabolism, excretion, and toxicity) parameters [47,48].

Method for Molecular Docking

The starting three-dimensional (3D) structure from Protein Data Bank (PDB) with ID: 2WTP was taken for docking [49]. After taking the proteins from PDB, these were viewed by the PyMOL software version V2.3 (https://pymol.org/2/) [50]. All water molecules and unexpected ligands or heteroatoms were removed to get fresh protein, and it was saved as PDB files. The PyRx software was used for molecular docking in the term of AutoDock Vina. After the molecular docking, the docked complexes were taken Discovery Studio version 2017 for result analyses and view [51].

Molecular Dynamic

To perform molecular dynamic (MD) simulations, NAMD software was used to run interactively with live view or in batch mode on a desktop computer [52]. MD simulation was devoted to underpining the docking best fitting and stability of ligand-protein completes up to 5000 ns for holo-form (drug-protein) applying AMBER14 force field [53]. In the presence of a water solvent, the total system was equilibrated with 0.9% NaCl at 298 K temperature. A cubic cell was propagated within 20 Å on every side of the process and periodic boundary circumstances during the simulation. After simulation, the root mean square deviation (RMSD) and root mean square fluctuation (RMSF) were analyzed using the visual molecular dynamics (VMD) software.

Calculation Inhibition Constant (IC_{50})

The software packet MGLtool 1.5.6 was used in the case of AutoDock Vina calculation with adding polar hydrogens and selective active site of protein. Using this tool, inhibition constant (μM), ligand efficiency, internal energy (kcal mol^{-1}), van der Waals-hydrogen bonding-desolvation energy (kcal mol^{-1}), electrostatic energy (kcal mol^{-1}), torsional energy (kcal mol^{-1}), and unbound energy (kcal mol^{-1}) were calculated for ligand-protein complex after docking.

Calculation of QSAR

The ChemoPy (python package) descriptors from ChemDes (chemical descriptors) database contain about 633 descriptors to explain the biological profiles [23]. Using a genetic search algorithm and cross-validated by using the leave-one-out cross-validation method, the following equation was developed where the most eight descriptors, correlated with biological activity and molecular dynamic study, were characterized. Using multi-linear regression (MLR) equations, the model was built to predict the quantitative structure-activity relationship (QSAR) [54].

Here, pIC_{50} (Activity) $= -2.768483965 + 0.133928895 \times (Chiv5) + 1.59986423 \times (bcutm1) + (-0.02309681) \times (MRVSA9) + (-0.002946101) \times (MRVSA6) + (0.00671218) \times (PEOEVSA5) + (-0.15963415) \times (GATSv4) + (0.207949857) \times (J) + (0.082568569) \times (Diameter)$.

RESULTS AND DISCUSSION

Synthesis and Optimized Structure of Glucofuranose 3-8

Initially, bisacetone D-glucose was prepared from

D-glucose, which was subjected to selective 5,6-*O*-isopropylidene deprotection and produced compound 3 (Fig. 2). Direct regioselective stearoylation of 3 under several reaction conditions gave 4. Stearoate 4 was then converted to 3,5-di-*O*-acylates 5-8 with four different acylating agents [42].

In computational chemistry, it is essential to determine the stable configuration of any molecular structure. The optimized structures of glucofuranoses 3-8, obtained from the DFT B3LYP functional and 6-31G++ basis set, are added in Fig. 3. The optimized structures of these molecules indicated that they have almost the same symmetry. These optimized stable structures are the root of all other computer aided studies.

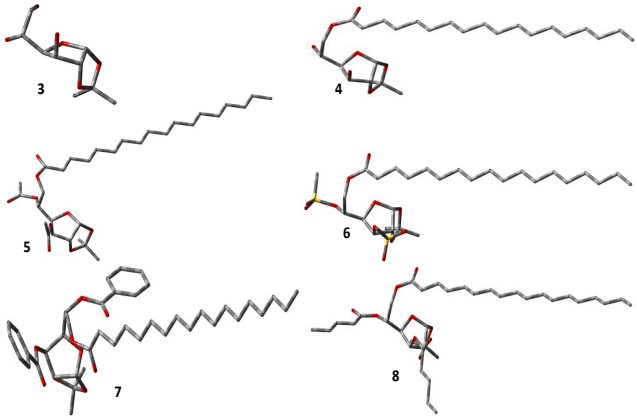

Fig. 3. DFT optimized structures of glucofuranose 3-8 (without H atoms).

Molecular Orbitals and Chemical Reactivity Descriptors

The chemical descriptors generally carry a special significance for any organic compound or biologically active molecule. The magnitude of εLUMO, εHOMO and energy gap (Δε), ionization potential (I), electron affinity (A), chemical potential (μ), electronegativity (χ), hardness (η), electrophilicity (ω) and softness (S) of the six molecules 3-8 are presented in Table 1. These data were calculated by DFT functions.

The smaller the energy gap Δε the greater the reactivity for a molecule. Here, the addition of ester group(s) gradually decreased Δε than the non-ester 3, and thus, these esters 4-8 can easily participate in chemical reactions [55-57]. The highest electrophilicity index ω value for 7 (13.573 eV) and 8 (15.534 eV) indicated them as stronger electrophiles among the compounds. From Table 1, it can be seen that the lowest value of softness is found for non-ester 3 (0.196 eV), whereas with the addition of ester groups, as in 4-8, its softness increased (~0.300 eV) and inversely hardness decreased. Overall, the ester compound's (4-8) hardness decreased by ~1.5-2.0 eV than the glucofuranose 3. Thus, according to the maximum hardness principle, these compounds 4-8 should be more reactive, should have better biological activity, and have greater acceptability to use as medicine against any pathogens [58,59].

Frontier Molecular Orbital: HOMO and LUMO

The DFT method has been used to determine the HOMO and LUMO orbital diagrams. HOMO generally refers to the maximum amount of electron density in the

Table 1. Frontier Molecular Orbitals and Reactivity Descriptor Analysis of 3-8

Mol	εLUMO (eV)	εHOMO (eV)	Δε (eV)	I (eV)	A (eV)	μ (eV)	η (eV)	χ (eV)	ω (eV)	S (eV)
3	-0.697	-10.902	10.205	10.90	0.697	-5.799	5.102	5.799	3.295	0.196
4	-1.595	-8.093	6.522	8.093	1.595	-4.844	3.249	4.844	3.611	0.307
5	-1.571	-7.774	6.203	7.774	1.571	-4.672	3.101	4.672	3.519	0.322
6	-1.311	-7.665	6.463	7.665	1.311	-4.488	3.177	4.488	3.169	0.314
7	-2.556	-5.856	1.701	5.856	2.556	-4.206	0.850	4.206	10.405	1.176
8	-7.705	-13.232	5.527	13.23	7.705	-10.468	3.527	10.468	15.534	0.283

Mol = molecule (compound); LUMO = lowest unoccupied molecular orbital; HOMO = highest occupied molecular orbital.

part of the molecule where an electrophile can easily attack. From the following pictures (Fig. 4), it can be seen that the HOMO part extends on the furanose and hydroxyl group. So, as these are electronegative atoms *i.e.* oxygen(s), those regions are more likely to have HOMO orbitals. This study clearly showed that this conceptual knowledge about HOMO from the frontier molecular orbital after analysis of their optimized structures. The term LUMO, on the other hand, refers to the lack of electrons where an electron withdrawing group or nucleophilic group can easily be added. From Fig. 4, it is seen that the LUMO of these molecules is associated in the alkyl group/part(s).

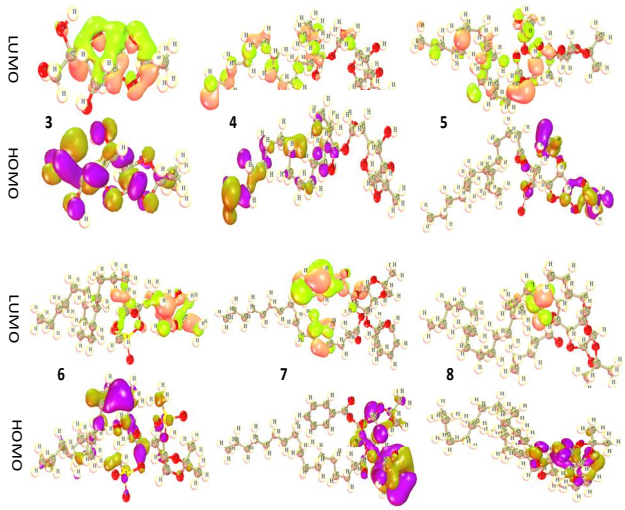

Fig. 4. Frontier molecular orbitals diagram for HOMO and LUMO of glucofuranose 3-8.

Pharmacokinetics: Drug-likeness Study

Christopher A. Lipinski proposed a well-known rule (rule of five) in 1997 for drug-like molecules based on the five parameters such as drug molecule should have- (i) less than 5 hydrogen bond donors (HBD), (ii) less than 10 hydrogen bond acceptors (HBA), (iii) more than three number of rotatable bonds (NBR), (iv) molecular mass (MW) less than 500 Daltons, and (v) octanol-water partition coefficient (logPo/w) is not greater than 5 [60]. The HBD, HBA, NBR, MW, logPo/w, and Lipinski rule violation of the glucofuranose compounds are presented in Table 2. It is found that almost all glucofuranose molecules 3-8 mostly obeyed the Lipinski rule. Also, these compounds (except mesylate 6) possess a topological polar surface area below140 Å². All these factors are in favor of better drug-likeness properties of these glucofuranose esters. It should be noted that for pharmacokinetic properties of all the compounds 3-8 are compared with standard antifungal drugs like fluconazole (9) and amphotericin B (10).

Pharmacokinetics: ADMET Studies

The bursting short form of ADMET is the absorption, distribution, metabolism, excretion, and toxicity which are estimated as the fundamental parts of any drug development program. In order to minimize the price tag and consumption of time, the prediction of ADME data helps to design a new drug molecule before the chemical synthesis

Table 2. Data of Lipinski Rule, Pharmacokinetics and Drug-likeness of 3-8

Mol	HBD	HBA	NBR	TPSA (Å²)	logPo/w	logKp (cm s^{-1})	Lipinski rule		MW	BS	GIA
							Result	Violation			
3	03	06	02	88.38	-0.54	-7.84	Yes	0	220.22	0.55	High
4	02	07	20	94.45	5.67	-3.62	Yes	0	486.68	0.55	High
5	0	09	24	106.59	6.56	-3.71	Yes	1	570.76	0.55	Low
6	0	11	24	157.49	6.01	-4.81	No	2	642.86	0.17	Low
7	0	09	26	224.56	8.76	-1.60	No	2	710.01	0.56	Low
8	0	09	30	106.59	8.52	-2.28	No	2	654.91	0.17	Low
9	01	09	05	26.71	0.66	-8.21	Yes	0	316.35	0.55	High
10	12	18	03	319.61	-0.65	-11.94	No	3	924.08	0.17	Low

Note: For rigorous comparison 9 (fluconazole) and 10 (amphotericin B) are included in the study; TPSA = topological polar surface area; logKp for skin permeation; BS = Bioavailability Score; GIA = gastrointestinal absorption.

and clinical trial phase. As a result, the situation of drug discovery has been changing rapidly and dramatically with the blessing of computational tools. Table 3 represents the data of ADME parameters of the glucofuranose molecules.

First of all, all molecules have a positive response to blood brain barrier, and it is opposite for CYP450 2C9 substrate and CYP450 1A2 inhibitor. The value of Caco-2 permeability is about from -0.7302 to -0.7880. Moreover, they can show the positive result for P-II glycoprotein substrate (except 6) and P-I glycoprotein inhibitor (except 3 and 6). Also, the subcellular localization for all tested molecules is found to be the mitochondria.

Toxicity. *In silico* techniques satisfy the increasing need for rapid safety assessment of chemicals for both industries and regulatory agencies, and are used throughout the world. The toxicity of the glucofuranose esters and standard drugs for acute and non-acute species, tested on rats and fish, were obtained by an online database for computational prediction, and are mentioned in Table 4.

It is observed that all drugs have more solubility in

Table 3. ADME Properties of 3-10

Mol	HIA	C2P	BBB	P-I GpI	P-II GpS	Renal OCT	Sub-cellular localization	CYP450 2C9 Substrate	CYP450 1A2 Inhibitor
3	0.5922	-0.7302	Yes	No	Yes	0.9388	Mitochondria	No	No
4	0.7222	-0.7308	Yes	Yes	Yes	0.9043	Mitochondria	No	No
5	0.8208	-0.7345	Yes	Yes	Yes	0.8673	Mitochondria	No	No
6	0.7609	-0.7858	Yes	No	No	0.8798	Mitochondria	No	No
7	0.9350	- 0.5728	Yes	Yes	Yes	0.7765	Mitochondria	No	No
8	0.8208	-0.7880	Yes	Yes	Yes	0.8673	Mitochondria	No	No
9	0.9079	-0.7320	Yes	No	Yes	0.5785	Mitochondria	No	No
10	0.9664	- 0.8681	No	No	Yes	0.9491	Mitochondria	No	No

HIA = human intestinal absorption; C2P = caco-2 permeability; BBB = blood brain barrier; GpI = glycoprotein inhibitor; GpS = glycoprotein substrate; OCT = organic cation transporter.

Table 4. Aquatic and Non-aquatic Toxicity

Mol	AMES toxicity	Carcin-ogenicity	Water solubility (logS)	Plasma protein binding	Acute oral toxicity (Kg mol^{-1})	ORA Toxicity (LD_{50}) (mol Kg^{-1})	Fish toxicity (pLC_{50}) (mg l^{-1})	*T. Pyriformis* toxicity (logμg l^{-1})
3	No	No	-0.801	0.179	2.464	1.9593	2.4984	-0.1810
4	No	No	-2.822	0.932	2.733	2.6187	1.6374	0.9125
5	No	No	-3.568	0.728	2.532	1.9834	0.8075	0.8324
6	No	No	-3.311	0.732	3.033	2.5040	1.3050	0.6288
7	No	No	-4.82	0.756	3.587	2.2031	-0.5120	1.1619
8	No	No	-3.568	0.757	2.485	1.9834	0.8075	0.8324
9	Yes	No	-2.292	0.720	3.033	2.5490	1.9190	0.2811
10	No	No	-3.091	0.653	3.013	2.2357	1.5706	0.4977

Mol = molecule (compound); ORA = oral rat acute.

water medium and possess variable values while compound 7 showed the highest tendency in water solubility (-4.82), and 10, 8, 6, and 5 stayed around -3.0 to -3.5. As a result, these samples (3 to 10) are conceptually toxic due to high water solubility where the pLC_{50} score is about 2.498310 to -0.3597 mg l^{-1} as aquatic species, especially fish. But, the positive and strong side of these carbohydrate drugs is their non-AMES toxicity and non-carcinogenicity. Again, the toxicity profiles of glucofuranose esters (4-8) are comparable to the standard drugs 9 and 10 (Table 4), and hence they are comparatively safe to use.

Molecular Docking Studies

The recent outbreak of mucormycosis, due to black fungus, showed symptoms like blackening or discoloration over the nose, blurred or double vision, chest pain, breathing difficulties, and coughing blood. Rhizopus, Mucor, and Lichtheimia (formerly Absidia) species are the most common members of the order Mucorales that cause mucormycosis, accounting for 70 to 80% of all cases which have been occurring in India during the SARS-CoV-2 pandemic. Among these, the *Rhizomucor miehei* species is the most powerful pathogen for causing mucormycosis. Thus, the *Rhizomucor miehei* protein [49] was selected for the study for evaluating their computational evaluations using molecular docking, QSAR, molecular dynamics (MD), and related studies.

Molecular docking studies were conducted to find the binding site of protein regarding the active site of the protein, and provide evidence for the binding affinity of drug compounds with protein as macromolecules [61,62]. As the protein-ligand interaction plays a significant role in structural based drug designing, the H bonds, halogen bonds, van der Waal bonds, and hydrophobic bonds are the main key factor for binding the active site of protein to form docking score as binding affinity where the docking score above 6.00 kcal mol^{-1} has been considered as a standard drug [62-64]. These predicted binding and docked energies are the sum of the intermolecular energy and the torsional free-energy, and the docking ligand's internal energy, respectively. In this perspective and due to the better antifungal nature of 4-8 [42] their binding affinities were calculated against mucormycosis' pathogens (black fungus; PDB ID: 2WTP; Table 5).

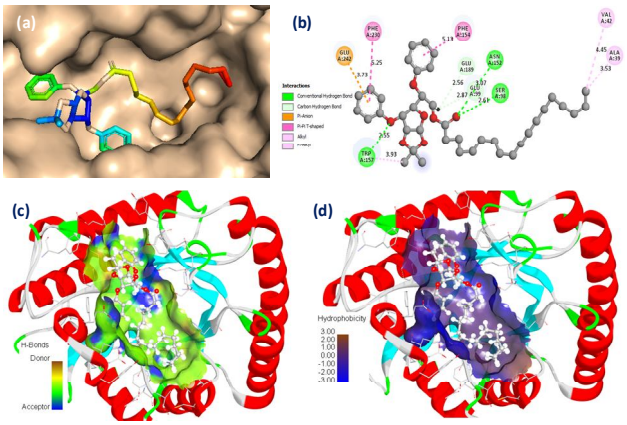

Fig. 5. Different docking pose for 8: (a) ligand in protein pocket; (b) 2D diagram of protein ligand interaction; (c) H bonding pose of protein ligand interaction; (d) hydrophobic bonding pose of protein ligand interaction.

It is seen that the binding affinity of 7 (-7.80 kcal mol^{-1}) and 8 (-8.20 kcal mol^{-1}) are higher than the standard value. For more specific study about these compounds, the standard antifungal drug fluconazole (9) was docked against the same protein and obtained the binding affinity in -6.50 kcal mol^{-1} which is also much lower than the value of 7 and 8 (Fig. 5) and is slightly lower than 4-6. In general, the binding affinities for auto docking of compounds 3-6 are about -6.02 to -6.80 kcal mol^{-1} which is found to be standard in terms of theoretical and conceptual docking protocol. Moreover, the number of hydrophobic bonds is greater than the number hydrogen of bonds except for 5 and 7. The standard Amphotericin B (10) showed the highest binding affinity (-10.00 kcal mol^{-1}).

Calculation of Inhibition Constant

In the case of molecular docking, five other parameters, such as inhibition constant (Ki), intermolecular energy, electrostatic energy, torsion energy, unbounded energy of docked protein-ligand complex were also determined by AutoDock tools. It should be noted that the Ki is directly proportional to binding energy, and theoretically, it is expressed as IC_{50}. The IC_{50} or inhibition constant demonstrated ranging from 16.04 to 58.66 μM (Table 6). The compounds 3-8 had a smaller value of inhibition

Table 5. Data of Binding Energy and Name of Interacted Ligand for Protease (2WTP)

Ligand	Binding affinity (kcal mol^{-1})	No. of H bond	No. of hydrophobic bond	No. of van der Waal bond	Total bonds
3	-6.02	05	06	Absent	11
4	-6.60	03	07	Absent	10
5	-6.80	06	02	Absent	08
6	-6.50	04	07	Absent	11
7	-7.80	03	04	Absent	07
8	-8.20	05	06	Absent	11
9	-6.50	03	02	01	06
10	-10.00	03	02	Absent	05

Table 6. Data from the Auto Dock Vina and Inhibition Constant

Ligand	Inhibitor constant (μM)	Ligand efficiency	IE (A)	EE	TIE (B)	TE (C)	UE (D)	BE
			(Kcal mol^{-1})					
3	58.66	-0.29	-5.88	-0.29	-2.56	1.49	-2.56	-4.39
4	42.65	-0.11	-10.30	-0.06	-2.76	6.56	-2.76	-3.73
5	22.77	-0.10	-11.08	0.01	-3.26	7.16	-3.26	-3.92
6	44.30	-0.11	-11.83	-0.02	-4.27	7.16	-4.27	-4.67
7	20.11	-0.11	-11.68	-0.10	-3.42	7.16	-3.22	-4.72
8	16.04	-0.10	-10.93	-0.23	-5.95	8.98	-5.95	-1.95
9	40.10	-0.11	-11.53	-0.12	-3.27	7.16	-3.27	-4.42
10	16.00	-0.10	-10.10	-0.20	-2.40	7.98	-4.40	-0.12

IE = intermolecular energy; EE = electrostatic energy; TIE = total internal energy; TE = torsional energy; UE = unbound energy; BE = binding energy.

constant where the standard value is 80.08 μM. In addition, the standard antifungal drug, fluconazole, had Ki value of 40.10 μM and binding energy of -4.42 kcal mol^{-1}. Finally, it could be said from the docking poses and docking scores obtained from Table 6 that the tested compound 7 and 8 are highly active molecules against black fungus.

The docking poses were ranked in keeping with their docking scores and both the ranked list of docked ligands and their corresponding binding pose [65]. The docking pose completely depends on the binding positions of the ligand with the enzyme shown in Fig. 5. Moreover, the binding energy of the individual compound was calculated using the formula: Binding energy = A + B + C - D [A = intermolecular energy + van der Waals energy (vdW) + hydrogen bonds + desolvation energy + electrostatic energy (kcal mol^{-1}); B = total internal energy (kcal mol^{-1}); C = torsional free energy (kcal mol^{-1}); D = unbound system's energy (kcal mol^{-1})]. Due to the close proportional relationship of binding energy and inhibitor constant, it is illustrated in Table 5 and found that the lower inhibitor constant has the lower binding energy. Thus, lower binding energy or inhibitor constant (20.11 and 16.04 μM) was obtained for both 7 and 8 which are lower (better) than the standard 9 and close to the standard 10.

Protein-ligands Interaction and Active Sites

In a protein, how many active sites of amino acid residues are present and, where they are associated with

drug or ligand is calculated by the Discovery Studio analysis. After the literature review of protein (2WTP) the active sites were found GLU-99, TRP-157, and TRP-65. First of all, auto docking was performed against the protein for getting the binding affinity and block of the binding site (Table 5). Analysis showed that all of the drugs selected were able to block active sites of amino acid residues GLU-99 and TRP-157 (Table 7), and the drugs could form strong hydrogen bonds with a lower bond distance (around 2.40 to 3.02 Å). Also, the residue TRP-157 has multiple weak hydrophobic bonds. Finally, it could be revealed from the binding interaction discussion regarding the binding pose and score that all selected compounds can show the high binding capacity of black fungus protein (2WTP) while the compounds 7 and 8 are superior to standard drug fluconazole (9). The hydrogen bond was created with the oxygen atom of ligand present in the side chain of furanose ring, and the hydrophobic bonds were created for non-polar ends, such as benzene ring and alkyl chain.

Table 7. Protein and Ligands Interaction with Amino Acid Residues and their Bond Distance

Compound (ligand)	Hydrogen bond		Hydrophobic bond		Van der Waals bond
	Interacting residue of amino acid	Distance (Å)	Interacting residue of amino acid	Distance (Å)	
3	GLU-189; GLU-189; GLU-189; GLU-99; SER-98	2.94; 2.17; 2.30; 2.40; 2.27	TRP-157; TRP-157; PHE-245; PHE-245; PHE-230; PHE-154	5.71; 4.70; 5.19; 3.71; 4.51; 3.85	Absent
4	GLU-99; GLU-99; GLU-99	2.55; 2.09; 3.02	TRP-65; TRP-65; TRP-157; PHE-245; PHE-230; PHE-230; PHE-154	2.50; 5.27 5.86; 4.02; 4.75; 4.88; 4.33	Absent
5	GLU-99; GLU-99; PHE-154; TPR-157; TPR-157; SER-98	2.36; 2.48; 2.57; 2.54; 1.91; 2.63	PHE-38; VAL-134	3.53; 4.35	Absent
6	TPR-157; TPR-157; TPR-157; GLU-99	2.66; 2.38; 2.99; 2.76	PHE-245; PHE-230; PHE-154; PHE-28; TPR-157; TPR-157; TPR-157	4.71; 4.53; 5.20; 4.48; 6.53; 4.47; 4.59	Absent
7	ARG-103; GLU-189	3.33; 3.76	ARG-103; TYR-102; GLU-99; PHE-38; ALA-39	5.03; 5.07; 3.45; 3.71; 3.52	Absent
8	GLU-189; GLU-99; ASN-152; SER-98; TRP-157	2.56; 2.87; 3.07; 2.61; 2.55	VAL-42; ALA-39; TRP-157; GLU-242; PHE-230; PHE-154	4.45; 3.53; 3.93; 3.73; 5.25; 5.13	Absent
9	GLU-99; GLU-99; GLU-99	2.51; 2.01; 1.83	GLU-189; PHE-38; GLU-189 (fluorine bond)	3.75; 5.56; 4.46	-
10	TYR-136; TYR-102; TYR-237	2.97; 3.37; 2.97	PHE-38; VAL-10	5.37; 4.73	Absent

Note. TRP = Tryptophan, ASP = Aspartic acid, GLU = Glutamic acid, LEU = Leucine, THR = Threonine, ASN = Asparagine, GLN = Glutamine, PHE = Phenylalanine, ILE = Isoleucine, ARG = Arginine, VAL = Valine, SER = Serine, PRO = Proline, GLY = Glycine, HIS = Histidine, LYS = Lysine, TRP = Trypsine, CYS = Cysteine, MET = Methionine.

Molecular Dynamics

The molecular dynamics (MD) imply various phases evaluating the force field study of molecular interaction and its stability. However, it is one of the superior ways to determine the stability of the protein-ligand complex after docking. After simulating the molecular dynamics, it informed about the RMSD and RMSF values in the protein-ligand complex. The universally accepted value of these two parameters is considered below 2.0 Å with any variable [66,67]. If more than that, then all these complexes lose their stability after entering the biological system, and it is considered as non-binder [68,69]. The RMSD was found that when there was no interaction between them, their value was close to 2.4 Å (Fig. 6a) and it was slightly decreased after the formation of the hydrogen bond ranging about 2.2 Å (Fig. 6c). Thus, it can be said that hydrogen bonding is not sufficiently responsible for their stability. In the second one, it stayed below around 0.7 Å in case of protein backbone interaction with amino acid residue interaction with respect to both time and amino acid skeleton. A similar trend was found for RMSF. However, all molecules are highly stable in protein ligand complex form in the water system.

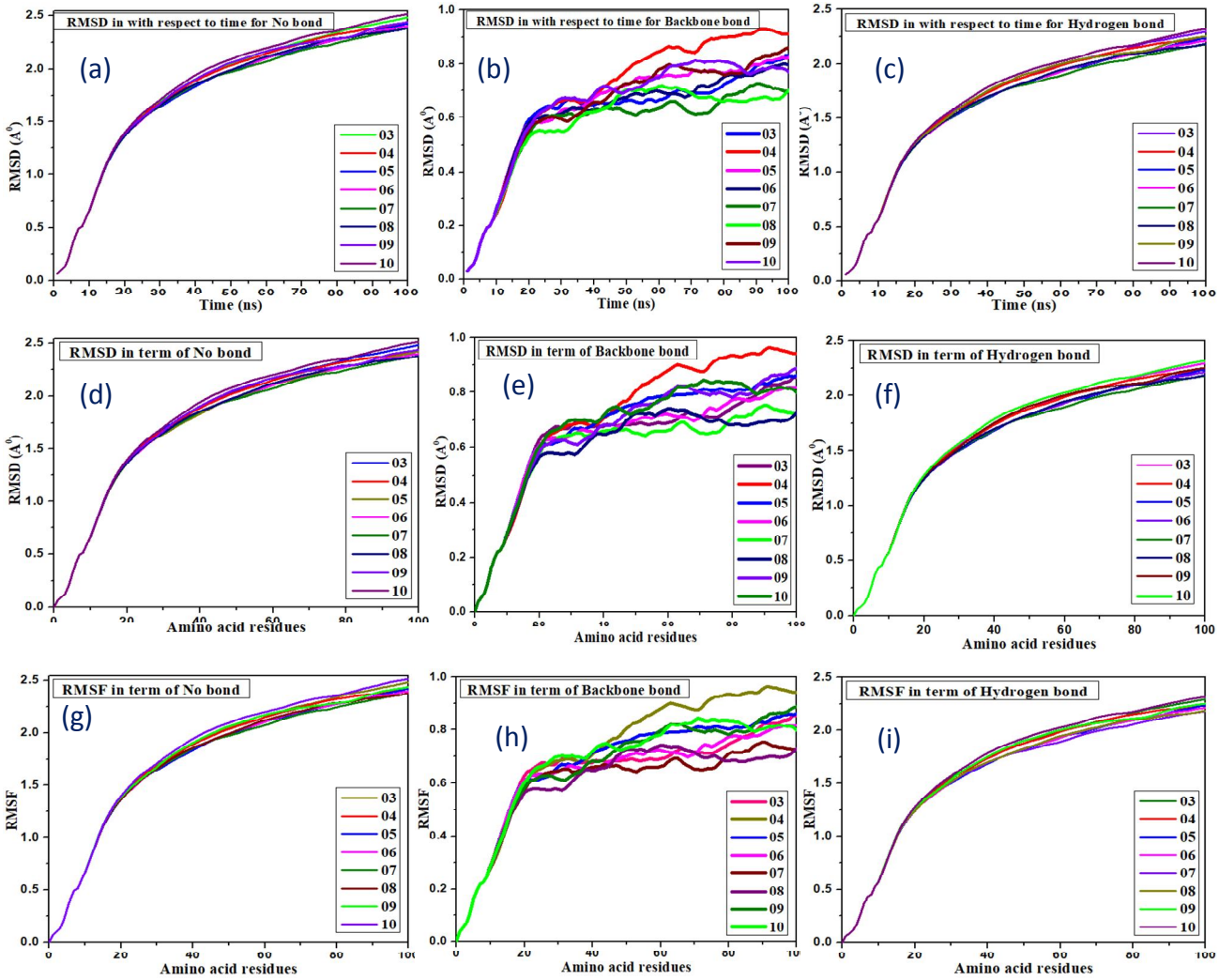

Fig. 6. Various graphs for protein *vs* compounds. RMSD: (a) Time *vs*. no bond; (b) Time vs protein skeleton; (c) Time *vs*. Hydrogen bond; (d) Amino acid *vs*. No bond; (e) Amino acid *vs*. back bond; (f) Amino acid *v*s. H bond. RMSF: (g) Amino acid *vs*. No bond; (h) Amino acid *vs*. back bond; (i) Amino acid *vs*. H bond.

Structure Activity Relationship (SAR)

The structure activity relationship (SAR) study is added to describe the most important outcome of this study. Based on the structural change(s) the compound 4-8 were designed by alkyl chain, mesyl, and benzoyl group with benzofuran for the replacement of hydroxyl group (furanose) and is considered the most powerful tool for evaluating the medicinal quantity of organic compound. The SAR of these compounds could be found, at first, in views of binding energy and binding affinity considering the 2D ligand-protein interactions. Standard compound 10 showed the highest binding affinity and binding energy among all other compounds, and the main reason is that there is a large alkyl chain. On the other hand, the sample 8 showed the highest binding energy and binding affinity due to its alkyl chain containing 17 carbon atoms and two 4-carbon alkyl groups. From the 2D structure of docking, it can be found that there are many hydrophobic bonds formed which are basically responsible to bind the protein more than the other compounds. This fact is also supported by the fact that compound 8 exhibited IC_{50} (16.04 μM) similar to standard amphotericin B (10, 16.0 μM). All other esters have higher binding affinity as compared to antifungal drug fluconazole (9). Thus, according to SAR, alkyl ester 8 might be the significant antifungal molecule. In the next step, this SAR phenomenon has been justified in terms of QSAR study with pIC_{50} values for specification.

QSAR and PlogIC_{50}

For mathematical and statistical relations of biological activity of drug molecules, quantitative structure-activity relationship (QSAR) plays a significant role in predicting the quantity of drug in a successful outcome for a drug design process. It had reported that a multiple linear regression-based statistical QSAR model was developed by evaluating the computational IC_{50} values from the ChEMBL database. This obtained IC_{50} value is the equivalent to pIC_{50} [-log(IC_{50})]. It is revealed that the ChEMBL was built by over a million chemical entities, and derived from the eight most acceptable biological descriptors, such as hiv5, bcutm1, MRVSA9, MRVSA6, PEOEVSA5, GATSv4, J, and diameter. In addition, the IC_{50} value is completely related to its structural chain and this value is changed with the change of its chain. With increasing the molecular mass, the value IC_{50} is increased but it must keep below 10.00 to become an effective drug. From Table 8, it has been found that the pIC_{50} is near 4.4424 to 7.5742. It is noted that the value of pIC_{50} for standard drugs is around 4.0 to 10. The drugs 3 and 9 showed the pIC_{50} around 4.450 which is considered the best drugs in terms of pIC_{50}.

CONCLUSIONS

The recent outbreak of black fungus along with COVID-19 deteriorated the pandemic situation. In this respect, several glucofuranose based sugar esters (SEs) having suitable molecular orbitals and chemical reactivity descriptors were docked against black fungus related protein 2WTP. The benzoyl (7) and pentanoyl (8) esters showed promising binding affinity and binding energy. Also, the inhibition constant (Ki or IC_{50}; 16.04 to 58.66 μM) of these compounds favors their anti-black fungal activities. The

Table 8. QSAR Parameters for 3-10

Drug	Chiv5	bcutm1	MRVSA9	MRVSA6	PEOEVSA5	GATSv4	J	Diameter	pIC_{50}
3	1.231	3.828	0.0	0.0	0.0	1.029	2.046	8.0	4.4424
4	3.203	3.835	5.969	0.0	96.815	1.015	1.374	26.0	6.5784
5	3.686	3.855	17.908	0.0	96.815	1.108	1.594	26.0	6.4303
6	4.659	4.602	26.206	0.0	96.815	1.146	1.672	26.0	7.5742
7	4.385	3.896	5.969	60.664	133.213	1.221	1.153	27.0	6.9036
8	4.133	3.86	17.908	0.0	123.504	1.274	1.75	28.0	6.8483
9	2.228	3.795	0.0	21.485	0.0	1.106	1.708	9.0	4.4598
10	4.918	3.853	11.939	85.064	98.912	0.862	1.710	25.0	6.4742

root mean square deviation (RMSD) and root mean square fluctuation (RMSF) of the compound-protein complex were found stable after 500 ns. These results in corroboration of their safe drug-likeness properties, especially for compounds 7 and 8, established these SEs as highly promising drug candidates for black fungus related diseases.

ACKNOWLEDGEMENTS

We are thankful to the Research and Publication Cell of the University of Chittagong, Bangladesh for a financial grant to accomplish this work (Special 2021, 124/5).

REFERENCES

[1] Roscales, S.; Plumet, J., Biosynthesis and biological activity of carbasugars. *Int. J. Carbohydr. Chem.* **2016**, e4760548, DOI: 10.1155/2016/4760548.

[2] Hevey, R., Strategies for the development of glycomimetic drug candidates. *Pharmaceut.* **2019**, *12*, 55, DOI: 10.3390/ph12020055.

[3] Ei-Laithy, H. M.; Shoukry. O.; Mahran, L. G., Novel sugar esters proniosomes for transdermal delivery of vinpocetine: Preclinical and clinical studies. *Eur. J. Pharm. Biopharm*. **2011**, *77*, 43-55, DOI: 10.1016/j.ejpb.2010.10.011.

[4] Dhavale, D. D.; Matin, M. M., Selective sulfonylation of 4-C-hyroxymethyl-β-L-threo-pento-1,4-furanose: Synthesis of bicyclic diazasugars. *Tetrahedron*, **2004**, *60*, 4275-4281, DOI: 10.1016/j.tet.2004.03.034.

[5] Dhavale, D. D.; Matin, M. M.; Sharma, T.; Sabharwal, S. G., Synthesis and evaluation of glycosidase inhibitory activity of octahydro-2H-pyrido[1,2-a]pyrimidine and octahydro-imidazo[1,2-a]pyridine bicyclic diazasugars. *Bioorg. Med. Chem.* **2004**, *12*, 4039-4044, DOI: 10.1016/ j.bmc.2004.05.030.

[6] Gumel, A. M.; Annuar, M. S. M.; Heidelberg, T.; Chisti, Y., Lipase mediated synthesis of sugar fatty acid esters. *Process Biochem.* **2011**, *46*, 2079-2090, DOI: 10.1016/j.procbio.2011.07.021.

[7] Matin, M. M.; Chakraborty, P.; Alam, M. S.; Islam, M. M.; Hanee, U., Novel mannopyranoside esters as sterol 14α-demethylase inhibitors: Synthesis, PASS predication, molecular docking, and pharmacokinetic studies. *Carbohydr. Res.* **2020**, *496*, e108130, DOI: 10.1016/j.carres.2020.108130.

[8] Teng, Y. L.; Stewart, S. G.; Hai, Y. W.; Li, X.; Banwell, M. G.; Lan, P., Sucrose fatty acid esters: Synthesis, emulsifying capacities, biological activities and structure-property profiles. *Critic. Rev. Food Sci. Nutr.* **2021**, *61*, 3297-3317, DOI: 10.1080/10408398.2020.1798346.

[9] Matin, M. M.; Bhattacharjee, S. C.; Chakraborty, P.; Alam, M. S., Synthesis, PASS predication, *in vitro* antimicrobial evaluation and pharmacokinetic study of novel n-octyl glucopyranoside esters. *Carbohydr. Res.* **2019**, *485*, e107812, DOI: 10.1016/j.carres.2019.107812.

[10] Matin, M. M.; Nath, A. R.; Saad, O.; Bhuiyan, M. M. H.; Kadir, F. A.; Abd Hamid, S. B.; Alhadi, A. A.; Ali, M. E.; Yehye, W. A., Synthesis, PASS-predication and *in vitro* antimicrobial activity of benzyl 4-O-benzoyl-α-L-rhamnopyranoside derivatives. *Int. J. Mol. Sci.* **2016**, *17*, e1412, DOI: 10.3390/ijms17091412.

[11] Perinelli, D. R.; Lucarini, S.; Fagioli, L.; Campana, R.; Vllasaliu, D.; Duranti, A.; Casettari, L., Lactose oleate as new biocompatible surfactant for pharmaceutical applications. *Eur. J. Pharm. Biopharm.* **2018**, *124*, 55-62, DOI: 10.1016/j.ejpb.2017.12.008.

[12] Islam, F.; Rahman, M. R.; Matin, M. M., The effects of protecting and acyl groups on the conformation of benzyl α-L-rhamnopyranosides: An in silico study. *Turkish Comp. Theo. Chem.* **2021**, *5*, 39-50. DOI: 10.33435/tcandtc.914768.

[13] Matin, M. M.; Iqbal, M. Z., Methyl 4-O-(2-chlorobenzoyl)-α-L-rhamnopyranosides: Synthesis, characterization, and thermodynamic studies. *Orbital Electron. J. Chem.* **2021**, *13*, 19-27, DOI: 10.17807/orbital.v13i1.1532.

[14] Demchenko, A. V., Stereoselective chemical 1,2-*cis* O-glycosylation: From 'Sugar Ray' to modern techniques of the 21st century. *Synlett.* **2003**, *2003*, 1225-1240, DOI: 10.1055/s-2003-40349.

[15] Crich, D., Chemistry of glycosyl triflates: Synthesis of β-mannopyranosides. *J. Carbohydr. Chem.* **2012**, *21*,

663-686, DOI: 10.1081/CAR-120016486.

[16] Matin, M. M.; Bhuiyan, M. M. H.; Debnath, D. C.; Manchur, M. A., Synthesis and comparative antimicrobial studies of some acylated D-glucofuranose and D-glucopyranose derivatives. *Int. J. Biosci.* **2013**, *3*, 279-287, DOI: 10.12692/ijb/3.8.279-287.

[17] Matin, M. M.; Bhuiyan, M. M. H.; Kabir, E.; Sanaullah, A. F. M.; Rahman, M. A.; Hossain, M. E.; Uzzaman, M., Synthesis, characterization, ADMET, PASS predication, and antimicrobial study of 6-O-lauroyl mannopyranosides. *J. Mol. Struct.* **2019**, *1195*, 189-197, DOI: 10.1016/j.molstruc.2019.05.102.

[18] Ren, B.; Zhang, L.; Zhang, M., Progress on selective acylation of carbohydrate hydroxyl groups. *Asian J. Org. Chem.* **2019**, *8*, 1813-1823, DOI: 10.1002/ajoc.201900400.

[19] Matin, M. M.; Sharma, T.; Sabharwal, S. G.; Dhavale, D. D., Synthesis and evaluation of glycosidase inhibitory activity of 5-hydroxy substituted isofagomine analogues. *Org. Biomol. Chem.* **2005**, *3*, 1702-1707, DOI: 10.1039/b418283a.

[20] Matin, M. M.; Chakraborty, P., Synthesis, spectral and DFT characterization, PASS predication, antimicrobial, and ADMET studies of some novel mannopyranoside esters. *J. Appl. Sci. Process Eng.* **2020**, *7*, 572-586, DOI: 10.33736/jaspe.2603.2020.

[21] Buzatu, A. R.; Frissen, A. E.; van den Broek, L. A. M.; Todea, A.; Motoc, M.; Boeriu, C. G., Chemoenzymatic synthesis of new aromatic esters of mono- and oligosaccharides. *Processes*, **2020**, *8*, e1638, DOI: 10.3390/pr8121638.

[22] Matin, M. M.; Hasan, M. S.; Uzzaman, M.; Bhuiyan, M. M. H.; Kibria, S. M.; Hossain, M. E.; Roshid, M. H. O., Synthesis, spectroscopic characterization, molecular docking, and ADMET studies of mannopyranoside esters as antimicrobial agents. *J. Mol. Struct.* **2020**, *1222*, e128821, DOI: 10.1016/j.molstruc.2020.128821.

[23] Richel, A.; Laurent, P.; Wathelet, B.; Wathelet, J-. P.; Paquot, M., Microwave-assisted conversion of carbohydrates. State of the art and outlook. *Comptes Rendus Chimie* **2011**, *14*, 224-234, DOI: 10.1016/j.crci.2010.04.004.

[24] Nilsson, H.; Andersen, J. E. T., New glucofuranose esters and glucopyranose esters of alkyl-fumarates useful for treating psoriasis and other hyperliferative, inflammatory and autoimmune disorders. **2007** (Patent No. WO2007006308-A1; EP1915387-A1; IN200800535-P2; EP1915387-B1).

[25] Rong, Y. W.; Zhang, Q. H.; Wang, W.; Li, B. L., A simple and clean method for O-isopropylidenation of carbohydrates. *Bull. Korean Chem. Soc.* **2014**, *35*, 2165-2168, DOI: 10.5012/bkcs.2014.35.7.2165.

[26] Lugiņina, J.; Vasiļjevs, D.; Ivanovs, I.; Mishnev, A.; Turks, M., Diastereoselective aza-Michael addition for synthesis of carbohydrate-derived spiropiperazinones. *Monatshefte für Chemie* **2019**, *150*, 21–28, DOI: 10.1007/s00706-018-2304-x.

[27] Matin, M. M., Synthesis of D-glucose derived oxetane: 1,2-O-Isopropylidene-4-(S)-3-O,4-C-methylene-5-O-methanesulfonyl-β-L-threo-pento-1,4-furanose. *J. Appl. Sci. Res.* **2008**, *4*, 1478-1482.

[28] Dhavale, D. D.; Matin, M. M., Piperidine homoazasugars: Natural occurrence, synthetic aspects and biological activity study. *ARKIVOC* **2005**, *2005*, 110-132, DOI: 10.3998/ark.5550190.0006.314.

[29] Catelani, G.; Osti, F.; Bianchi, N.; Bergonzi, M. C.; D'Andrea, F.; Gambari, R., Induction of erythroid differentiation of human K562 cells by 3-O-acyl-1,2-O-isopropylidene-D-glucofuranose derivatives. *Bioorg. Med. Chem. Lett.* **1999**, *9*, 3153-3158, DOI: 10.1016/s0960-894x(99)00547-8.

[30] Ridley, D. D.; Smal, M. A., Preparation of arenesulfinic esters of 1,2:5,6-di-O-cyclohexylidene-α-D-glucofuranose, and their conversion into optically active sulfoxide. *Austr. J. Chem.* **1982**, *35*, 495-507, DOI: 10.1071/CH9820495.

[31] Sheville, J.; Berndt, D.; Wagner, T.; Norris, P., Crystal structure of 1,2;5,6-di-O-isopropylidene-3-O-(phenylacetyl)-D-glucofuranose. *J. Chem. Cryst.* **2003**, *33*, 409-412, DOI: 10.1023/A:1024234231567.

[32] Matin, M. M.; Bhuiyan, M. M. H.; Azad, A. K. M.S.; Bhattacharjee, S. C.; Rashid, M. H. O., Synthesis and antimicrobial studies of 6-O-lauroyl-1,2-O-isopropylidene-α-D-gluco-furanose derivatives. *Chem. Biol. Interface* **2014**, *4*, 223-231.

[33] Matin, M. M.; Islam, N.; Siddika, A.; Bhattacharjee,

S. C., Regioselective synthesis of some rhamnopyranoside esters for PASS predication, and ADMET studies. *J. Turkish Chem. Soc. Sect. A: Chem.* **2021**, *8*, 363-374, DOI: 10.18596/jotcsa.829658.

[34] Matin, M. M.; Uzzaman, M.; Chowdhury, S. A.; Bhuiyan, M. M. H., *In vitro* antimicrobial, physicochemical, pharmacokinetics, and molecular docking studies of benzoyl uridine esters against SARS-CoV-2 main protease. *J. Biomol Struct. Dyn.* DOI: 10.1080/07391102.2020.1850358; PMID: 33297848; PMCID: PMC7738211.

[35] Ali, M.; Karim, M. H.; Matin, M. M., Efficient synthetic technique, PASS predication, and ADMET studies of acylated n-octyl glucopyranosides. *J. Appl. Sci. Process Eng.* **2021**, *8*, 648-659, DOI: 10.33736/jaspe.2823.2021.

[36] Najafzadeh, M. J.; Vicente, V. A.; Sun, J.; Meis, J. F.; de Hoog, G. S., Fonsecaea multimorphosa sp. nov, a new species of Chaetothyriales isolated from a feline cerebral abscess. *Fungal Biol.* 2011, *115*, 1066-1076, DOI: 10.1016/j.funbio.2011.06.007.

[37] McGinnis, M. R.; Hilger, A. E., Infections caused by black fungi. *Arch. Dermatol.* **1987**, *123*, 1300-1302, DOI: 10.1001/archderm.1987.01660340062020.

[38] Seneviratne, C. J.; Fong, P. H.; Wong, S. S.; *et al.* Antifungal susceptibility and phenotypic characterization of oral isolates of a black fungus from a nasopharyngeal carcinoma patient under radiotherapy. *BMC Oral Health* **2015**, *15*, 39, DOI: 10.1186/s12903-015-0023-9.

[39] https://www.bbc.com/news/world-asia-india-57027829

[40] https://www.bbc.com/future/article/20210519-mucormycosis-the-black-fungus-hitting-indias-covid-patients

[41] https://medcraveonline.com/JBMOA/JBMOA-09-00298.pdf

[42] Matin, M. M., Bhuiyan, M. M. H.; Azad, A. K. M. S.; Rashid, M. H.O., Synthesis of 6-O-stearoyl-1,2-O-isopropylidene-α-D-gluco-furanose derivatives for antimicrobial evaluation. *J. Physical Sci.* **2015**, *26*, 1-12.

[43] Delley, B., DMol, a standard tool for density functional calculations: review and advances, in: Theoretical and Computational Chemistry. Elsevier: **1995**, 2nd Ed., pp. 221-254.

[44] Delley, B., Time dependent density functional theory with DMol^3. *J. Phys.: Condens. Matter*. **2020**, *22*, 384208, DOI: 10.1088/0953-8984/22/38/384208.

[45] Islam, M. J.; Kumer, A.; Paul, S.; Sarker, M. N., The activity of alkyl groups in morpholinium cation on chemical reactivity, and biological properties of morpholinium tetrafluroborate ionic liquid using the DFT method. *Chem. Method.* **2020**, *4*, 130-142, DOI: 10.33945/SAMI/CHEMM.2020.2.3.

[46] Daina, A.; Michielin, O.; Zoete, V., SwissADME: A free web tool to evaluate pharmacokinetics, drug-likeness and medicinal chemistry friendliness of small molecules. *Sci. Rep.* **2017**, *7*, 1-13, DOI: 10.1038/srep42717.

[47] Cheng, F.; Li, W.; Zhou, Y.; Shen, J.; Wu, Z.; Liu, G.; Lee, PW.;, Tang, Y., AdmetSAR: a comprehensive source and free tool for assessment of chemical ADMET properties. *J. Chem. Inf. Model.* **2012**, *52*, 3099-3105, DOI: 10.1021/ci300367a.

[48] Yang, H.; Lou, C.; Sun, L.; Li, J.; Cai, Y.; Wang, Z.; Li, W.; Liu, G.; Tang, Y., AdmetSAR 2.0: web-service for prediction and optimization of chemical ADMET properties. *Bioinformatics* **2019**, *35*, 1067-1069, DOI: 10.1093/bioinformatics/bty707.

[49] Qin, Z.; Yan, Q.; Lei, J.; Yang, S.; Jiang, Z.; Wu, S., The first crystal structure of a glycoside hydrolase family 17 β-1,3-glucanosyltransferase displays a unique catalytic cleft. *Acta Crystallogr. D Biol. Crystallogr.* **2015**, *71*, 1714-1724, DOI: 10.1107/S1399004715011037.

[50] DeLano, W. L., The PyMOL user's manual. 2002. http://www.pymol.org

[51] AS Inc. Discovery Studio Modeling Environment, Release 4.0., **2013**.

[52] Phillips, J. C.; Hardy, D. J.; Maia, J. D.C.; Stone, J. E.; Ribeiro, J. V., *et al*. Scalable molecular dynamics on CPU and GPU architectures with NAMD. *J. Chem. Phys.* 2020, *153*, e044130, DOI: org/10.1063/5.0014475.

[53] Skjevik, A. A.; Madej, B. D.; Dickson, C. J.; Teigen, K.; Walker, R. C.; Gould, I. R., All-atom lipid bilayer

self-assembly with the AMBER and CHARMM lipid force fields. *Chem. Comm*. **2015**, *51*, 4402-4405, DOI: 10.1039/C4CC09584G.

[54] De Oliveira, D. B.; Gaudio, A. C., BuildQSAR: a new computer program for QSAR analysis. *Mol. Informatics,* **2001**, *19*, 599-601, DOI: 10.1002/1521-3838.

[55] Ajoy, K.; Ahmed, M. B.; Sharif, M.; Al-Mamun, A.; Abdullah, M., A theoretical study of aniline and nitrobenzene by computational overview. *Asian J. Phys. Chem. Sci.* **2017**, *4*, 1-12, DOI: 10.9734/AJOPACS/2017/38092.

[56] Kumer, A.; Paul, S.; Zannat, A., The theoretical prediction of thermophysical properties, HOMO, LUMO, QSAR and biological indics of cannabinoids (CBD) and tetrahhdrocannabinol (THC) by computational chemistry. *Adv. J. Chem. Sect. A*, **2019**, *2*, 190-202, DOI: 10.33945/SAMI/AJCA.2019.2.190202.

[57] Hanee, U.; Rahman, M. R.; Matin, M. M., Synthesis, PASS, in silico ADMET, and thermodynamic studies of some galactopyranoside esters. *Phys. Chem. Res.* **2021**, *9*, 591-603, DOI: 10.22036/pcr.2021.282956.1911.

[58] Hoque, M. M. H.; Sajib, M.; Kumer, A.; Khan, M. W., Synthesis of 5,6-diaroylisoindoline-1,3-dione and computational approaches for investigation on structural and mechanistic insights by DFT. *Mol. Simulation* **2020**, *46*, 1298-1307, DOI: 10.1080/08927022.2020.1811866.

[59] Kumer, A.; Sarker, M. N.; Paul, S., The theoretical investigation of HOMO, LUMO, thermophysical properties and QSAR study of some aromatic carboxylic acids using HyperChem programming. *Int. J. Chem. Tech*. **2019**, *3*, 26-37, DOI: 10.32571/ijct.478179.

[60] Lipinski, C. A.; Lombardo, F.; Dominy, B. W.; Feeney, P. J., Experimental and computational approaches to estimate solubility and permeability in drug discovery and development settings. *Adv. Drug Deliv. Rev.* **2001**, *46*, 3-26, DOI: 10.1016/s0169-409x(00)00129-0.

[61] Hornig, H.; Woolley, P.; Lührmann, R., Decoding at the ribosomal A site: antibiotics, misreading and energy of aminoacyl-tRNA binding. *Biochimie*, **1987**, *69*, 803-813, DOI: 10.1016/0300-9084(87)90207-0.

[62] Babahedari, A. K.; Soureshjani, E. H.; Shamsabadi, M. K.; Kabiri, H., The comprehensive evaluation docking of methicillin drug containing isoxazole derivatives, as targeted antibiotics to Staphylococcus aureus. *J. Bionanoscience* **2013**, *7*, 88-291, DOI: 10.1166/jbns.2013.1119.

[63] Cheng, K.; Zheng, Q-. Z.; Qian, Y.; Shi, L.; Zhao, J.; Zhu, H-. L., Synthesis, antibacterial activities and molecular docking studies of peptide and Schiff bases as targeted antibiotics. *Bioorg. Med. Chem*. **2009**, *17*, 7861-7871, DOI: 10.1016/j.bmc.2009.10.037.

[64] Hermann, T.; Westhof, E., Docking of cationic antibiotics to negatively charged pockets in RNA folds. *J. Med. Chem.* **1999**, *42*, 1250-1261, DOI: 10.1021/jm981108g.

[65] Madeswaran, A.; Umamaheswari, M.; Asokkumar, K., *et al.* Discovery of potential aldose reductase inhibitors using in silico docking studies. *Orient. Pharm. Expt. Med*. **2012**, *12*, 157-161, DOI: 10.1007/s13596-012-0065-3.

[66] Bertamino, A.; Iraci, N.; Ostacolo, C.; Ambrosino, P.; Musella, S.; *et al.* Identification of a potent tryptophan-based TRPM8 antagonist with in vivo analgesic activity. *J. Med. Chem*. **2018**, *61*, 6140-6152, DOI: 10.1021/acs.jmedchem.8b00545.

[67] Talarico, C.; Gervasoni, S.; Manelfi, C.; Pedretti, A.; Vistoli, G.; Beccari, A. R., Combining molecular dynamics and docking simulations to develop targeted protocols for performing optimized virtual screening campaigns on the HTRPM8 channel. *Int. J. Mol. Sci.* **2020**, *21*, 2265, DOI: 10.3390/ijms21072265.

[68] Liu, K.; Kokubo, H., Exploring the stability of ligand binding modes to proteins by molecular dynamics simulations: a cross-docking study. *J. Chem. Inform. Model.* **2017**, *57*, 2514-2522, DOI: 10.1021/acs.jcim.7b00412.

[69] Guterres, H.; Im, W., Improving protein-ligand docking results with high-throughput molecular dynamics simulations. *J. Chem. Inform. Model.* **2020**, *60*, 2189-2198, DOI: 10.1021/acs.jcim.0c00057.